IN-35
21392
p 11

NASA Technical Memorandum 104481

Particle Displacement Tracking Applied to Air Flows

Mark P. Wernet
Lewis Research Center
Cleveland, Ohio

Prepared for the
Fourth International Conference on Laser Anemometry
cosponsored by the American Society of Mechanical Engineers and the European Association for Laser Anemometry with organizational collaboration and sponsorship from Case Western Reserve University, Cleveland State University, NASA Lewis Research Center, and the Ohio Aerospace Institute
Cleveland, Ohio, August 5–9, 1991

NASA

PARTICLE DISPLACEMENT TRACKING APPLIED TO AIR FLOWS

Mark P. Wernet

NATIONAL AERONAUTICS AND SPACE ADMINISTRATION
Lewis Research Center
Cleveland, OH 44135

ABSTRACT

Electronic Particle Image Velocimetric (PIV) techniques offer many advantages over conventional photographic PIV methods such as fast turn around times and simplified data reduction. A new all electronic PIV technique has been developed which can measure high speed gas velocities. The Particle Displacement Tracking (PDT) technique employs a single cw laser, small seed particles (1 μm), and a single intensified, gated CCD array frame camera to provide a simple and fast method of obtaining two-dimensional velocity vector maps with unambiguous direction determination. Use of a single CCD camera eliminates registration difficulties encountered when multiple cameras are used to obtain velocity magnitude and direction information. An 80386 PC equipped with a large memory buffer frame-grabber board provides all of the data acquisition and data reduction operations. No array processors or other numerical processing hardware are required. Full video resolution (640×480 pixel) is maintained in the acquired images, providing high resolution video frames of the recorded particle images. The time between data acquisition to display of the velocity vector map is less than 40 seconds. The new all electronic PDT technique is demonstrated on an air nozzle flow with velocities < 150 m/s.

INTRODUCTION

Particle Imaging Velocimetry (PIV) is a very useful tool for the study of fluid flow phenomena across a wide class of engineering applications. The traditional electro-mechanical beam readout PIV data reduction technique[1] is cumbersome, time consuming, and requires specialized array processors. The PDT technique described here is an all electronic data acquisition and data reduction technique for high velocity flows (0.1 m/s < v < 150 m/s) which has simple hardware requirements and provides fast data acquisition and reduction times. The new high speed PDT technique is a modified version of a previous low speed multiple image particle tracking technique, which was only applicable to low velocity liquid flows.

In PIV, pulsed light sheets are used to record the in-plane positions of particles entrained in the flow at two instances in time.[1] Low particle concentrations are used to ensure that individual particle images are clearly resolved.[2] Subsequent processing of the photographically recorded particle images yields a 2-D velocity vector map across an extended planar cross section of the flow. A common data reduction technique is the beam readout technique.[3,4,5] Other data reduction techniques involve digitizing small sections of the photograph and performing numerically intensive computations or employ image processors to detect velocity vectors.[6,7,8] All of the photographic recording PIV techniques offer high precision estimates of velocity (≈1%), but offer processing times measured in hours even on specialized array processors.

Other PIV work has focused on developing all electronic acquisition and processing systems. Electronic recording and processing offers the advantage of system integration, simplicity, and reduced processing times. In an electronic PIV system, all of the data acquisition and processing can be performed on a single computer. No media conversion is required. The comparatively low resolution of video cameras to that of photographic film limits the spatial resolution of electronic PIV recording techniques. However, if small (50×50 mm) cross sections of the flow are imaged, the spatial resolution of video cameras is acceptable.

A majority of the electronic PIV work has been concerned with resolving individual particle images and/or particle streaks. In some of the previous electronic PIV work, an asymmetric combination of particle streaks and dots were digitally recorded and later image processed to estimate streak lengths and dot spacings.[9,10,11] The velocity vector direction was determined from the asymmetry of the exposure pattern.

Time sequences of particle images to estimate velocity have been previously proposed and analyzed in computer simulations.[12,13,14] Cross-correlation and FFT techniques were used to obtain velocity magnitude, which are both computationally intensive operations. The cross-correlation technique yields the velocity vector direction information in conjunction with the vector magnitude. In the FFT approach, the sequence of single exposure particle image frames are linearly superimposed to generate a single multiple exposure record, which is then Fast Fourier Transformed to estimate the velocity vector magnitude. The sequence of single exposure images is used as a phase reference, so that the direction information can be resolved.

The high speed Particle Displacement Tracking (PDT) technique was developed from a low speed version of the PDT technique which used a sequence of five video fields to estimate the particle velocity magnitudes and directions.[15,16,17] In the low speed PDT technique, the maximum measurable velocity was 20 cm/s for a 50×50 mm field of view. The technique was limited by the RS-170 video field interval of

1/60 second. By slightly modifying the recording process, while maintaining the essential nature of the data reduction process, the PDT technique has been extended to enable directionally resolved measurements of high speed flows using standard RS-170 video signals.

Typically, multiple exposures are required per video frame when using an RS-170 compatible video format for data acquisition of high velocity flows (>1 m/s). To resolve the velocity vector direction unambiguously, the exposure sequence must be asymmetric, or consist of streaks and dashes.[8,9,10,11] Unfortunately, these long complex exposure patterns reduce the available information storage capacity of the video images. Recorded particle trajectories begin to cross and overlap, complicating the data reduction process and ultimately limiting the number of velocity vectors which may be resolved on a video image.

In the high speed PDT technique, only two exposures per video frame are used. However, two adjacent video frames are recorded, for a total of four exposures. The first two exposures occur on frame #1, near the end of the video frame integration period (1/30 second). The second two exposures occur on frame #2, near the beginning of the video frame integration period. Hence, two pairs of time separated particle images are recorded, which straddle the RS-170 video frame transfer interval. Time separating the particle image pairs allows unambiguous determination of the velocity vector direction. An intensified, gated CCD frame transfer camera is used to provide full resolution 640×480 square pixel images. The light sheet illumination is provided by a cw laser. All data acquisition and processing are performed using a single 80386 PC equipped with a large memory buffer frame-grabber board. No array processors are required and processing times are measured in terms of seconds from the time of image acquisition. Results obtained from applying the high speed PDT technique to a sonic nozzle flow seeded with 1 μm PSL seed particles will be presented.

PARTICLE DISPLACEMENT TRACKING

The Particle Displacement Tracking (PDT) technique is applicable to moderate to transonic velocity ($0.1 \leq V \leq 150$ m/s), sparsely seeded PIV fluid flow systems. In the PDT system, a cw laser source is used to generate a light sheet, and a gated, intensified, CCD frame camera connected to a frame-grabber board records the particle image data. A complete video frame is acquired every 1/30 second and consists of two interlaced video fields. Contrary to most traditional PIV setups, the laser source is operated in continuous wave mode, and the camera is gated via an externally supplied TTL pulse train. The pulse train is designed to enable the intensifier in the camera two times just at the end of video frame #1, and two more times at the beginning of video frame #2. A constant time interval (ΔT) is used between all of the enabling pulses. The actual value of ΔT is selected according to the fluid velocities of interest. The particle seeding number density is selected so that the individual particle images are clearly imaged, and the recorded particle images do not overlap.

The two video frames are then individually processed to determine the centroid location of all of the particle images. The particle centroid information is sufficient to determine the displacement of the particles between exposures. The particle image amplitude and shape information are used in estimating the centroids and then discarded. The particle image centroids are estimated to within $\pm \frac{1}{2}$ pixel.[15] Although the particle positions are actually estimated to sub-pixel accuracy, at this point in the PDT development the need for high precision particle position estimates is not required. A simple boundary following algorithm is used to identify the individual particle images. Each particle image mean centroid is computed using the particle image light intensity distribution. The details of the centroid processing and estimation are discussed in reference 15. The single pixel particle centroid estimates from all of the particle images recorded in the two frames are combined into a single 640×480×8 bit binary file. The time history of each particle image is encoded in the amplitude of the pixel marking the position of the particle centroid. The pixel amplitudes are coded according to the time order in the two frames. All of the particle centroids from video frame #1 are encoded into the composite image as pixels with amplitudes 2^1. Similarly, particle centroids from video frame #2 are encoded with amplitude 2^2. By amplitude coding the pixel locations of the particle centroids, a single image is generated which contains the time history displacements of all the particles recorded in the two frame sequence over a total time interval of $3\Delta T$. Figure 1 shows two particle image displacement records encoded into a 100×100 pixel image.

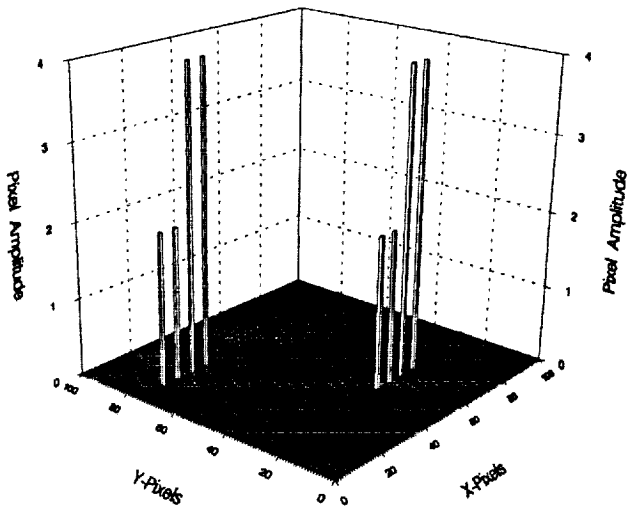

Figure 1: Time history coded particle centroids. Pixels with amplitude 2^1 were recorded on frame #1 and pixels with amplitude 2^2 were recorded on frame #2.

The amplitudes of the pixels marking the centroid positions are 2^1 at T=0 & $1\Delta T$, and 2^2 at T=$2\Delta T$ & $3\Delta T$. To aid in clarifying the particles according to their order of exposure in the four exposure sequence, the labels 2^1_1, 2^1_2, 2^2_3, and 2^2_4 will be used, where the superscripts denote which frame the particle centroid is from and the subscript denotes the exposure number in the four exposure sequence. Amplitude coding unambiguously defines the particle's direction of travel. The amplitude coding also decreases the probability of mistakenly

identifying a particle image from a different particle as being part of another particle displacement record. The number of crossed particle tracks is reduced by recording only two exposures per frame. Also, higher particle densities can be tolerated without a significant increase in the error rate of identification.

The essence of the PDT algorithm is to find the 2_2^1 and 2_3^2 amplitude pixels from the same particle and use the distance and angle between them to project where the 2_1^1 and 2_4^2 amplitude pixels are located. If all four pixels are detected in the appropriate order, then a valid velocity vector has been detected.

The time history image serves as the input to the PDT algorithm. The PDT algorithm begins by scanning the time history image and storing the locations of all pixels with amplitude 2^1, which corresponds to all particle positions on frame #1 (particles 2_1^1 and 2_2^1).

For each 2^1 amplitude particle position, a circular search region is defined around the pixel. Inside the search region, the coordinates of all pixels with amplitudes equal to 2^2 are scanned and stored. The 2^2 amplitude coded pixels correspond to the particle positions at both T=2ΔT & 3ΔT. The detected 2^2 amplitude pixels within the search region are now each successively analyzed. The distance and angle between each 2^2 amplitude pixel and the search region center 2^1 amplitude pixel is computed and used to project where the 2_1^1 and 2_4^2 amplitude pixels are located; see figure 2.

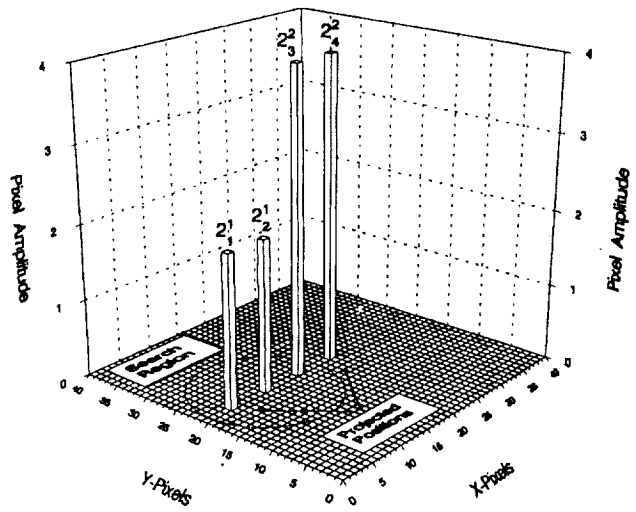

Figure 2: The PDT technique uses a circular search region to determine the particle displacement between exposures. The projected pixel locations must occur within the 3×3 search regions.

If the projected pixel locations for the 1st, and 4th particle images contain the correct amplitudes (2^1, and 2^2, respectively) then a complete particle displacement record has been detected. The velocity vector associated with this particle is computed from the distance between the initial and final particle locations (2_1^1 and 2_4^2 amplitude pixels), and the sum of the three inter-exposure intervals (3ΔT). The detected particle pixel amplitudes are then set to zero. If the projected particle locations detect the incorrect pixel amplitude or zero amplitude, then the 2^2 amplitude pixel within the search region is not the actual third image of the 2^1 amplitude pixel at the center of the search region. Each 2^2 amplitude pixel within the search region is examined until a complete particle displacement pattern is detected, or all of the 2^2 amplitude pixels are exhausted. If no match is found, the algorithm continues on to the next initial particle position 2^1 amplitude pixel. Remember that the 2^1 amplitude pixel being examined may be the 2_1^1 amplitude pixel, which will not have the corresponding 2_3^2 amplitude pixel adjacent to it. In summary, for each 2^1 amplitude pixel, a circular search region is defined about that particle, which is assumed to be the 2_2^1 particle. All 2^2 amplitude pixels within the search region are assumed to be the position of the particle at the third exposure (2_3^2), and thus used to predict the locations of the particle at time sequence exposures 1 and 4. No preknowledge about the flow system is required. The PDT system assumes that 2^2 amplitude pixels in the neighborhood of the 2^1 amplitude pixel are the most probable particle displacements between video frames #1 and #2. The maximum allowable particle displacement between exposures has previously been determined to be 10 pixels for sharply turning flows[15], or longer for 1-D flows. Ten pixel displacements between exposures minimizes the deviation of the particle path from a linear trajectory. Therefore, the search region size is defined to be a circle of radius 10 pixels; see figure 2.

The positioning error on the discrete grid must be accommodated in the PDT processing. As previously mentioned, the boundary processing technique provides particle centroid estimates to within ± ½ pixel on the 640×480 pixel time history image. For each projected particle position (for exposures 1 and 4) a 3×3 pixel search region is defined. The 3×3 search regions are centered on the projected positions; see figure 2. The expanded regions allow for the positioning error of ± ½ pixel. However, when a complete particle displacement pattern is detected, the exact location of the amplitude coded pixel within the 3×3 region is determined and used to determine the velocity vector magnitude. The velocity vector angle is computed from the position of the 2_1^1 and 2_4^2 amplitude pixels.

The random locations of independent particle images on the time history image frame can be misconstrued as originating from a single particle, which results in a false velocity vector identification. The main factors affecting the number of false identifications are the recorded particle number density and the circular search region radius. The particle arrival rate in the light sheet is Poisson. Assuming that the particle images are uniformly distributed across the recorded image and that the particle number density on each frame is the same, then the expected number of false identifications is given by the product of the number of initial search particles (pixel amplitude = 2^1), the number of 2^2 amplitude pixels in each circular search region, and the probabilities of particles being located within the two projected 3×3 search regions:

$$\langle V_f \rangle = N\pi r^2 \overline{\rho}^2 \varepsilon_p^4 \cdot \left[1 - e^{-\overline{\rho}\pi\varepsilon_p^2}\right]^2 \qquad (1)$$

where: $\langle V_f \rangle$ Expected number of false identifications
N Total number of pixels in recorded image
$\bar{\rho}$ Average particle number density in a frame
r User specified circular search region radius
ε_p^2 Pixel area

The average particle number density $\bar{\rho}$ recorded on frames #1 and #2 are twice as large as the number of particles actually present, due to the double exposure per frame.

There are two sources of error in the PDT estimated velocities: 1) the particle positioning error; and 2) the time interval error. The major source of error is from the particle centroid estimates. The total relative error in the measured velocity is given by:[15]

$$\frac{\sigma_U}{U} = \sqrt{\left(\frac{\sigma_X}{X}\right)^2 + \left(\frac{\sigma_T}{T}\right)^2} \qquad (2)$$

where U is the estimated mean velocity magnitude, X is the total particle displacement from the first to last exposures, T is the sum of the three inter-exposure intervals $3\Delta T$, σ_X is the rms error in the total particle displacement, and σ_T is the timing error. For the $\pm \frac{1}{2}$ pixel positioning error, the rms error in the total displacement is simply $1/\sqrt{2}$ pixels. The exposure pulse train is produced using an arbitrary waveform generator with a clock period resolution of 5 nsec.[18] An estimate for the time interval error is one clock period per exposure, or 4×5 nsec. Hence, for a 30 pixel total displacement and a total time interval of 30 μsec, the relative error in the estimated velocity is:

$$\frac{\sigma_U}{U} = \sqrt{\left(\frac{1/\sqrt{2}}{30}\right)^2 + \left(\frac{20\text{nsec}}{30\mu\text{sec}}\right)^2} \qquad (3)$$

or

$$\frac{\sigma_U}{U} = 0.024$$

which is dominated by the positioning error.

The error in the estimated velocity vector angle is similar to the magnitude error. The angular error is given by:[15]

$$\sigma_\theta = \tan^{-1}\left[\frac{1/\sqrt{2}}{30}\right] \qquad (4)$$

where X and σ_X are the particle displacement and rms error in the particle displacement, respectively. Using the same displacement of 30 pixels, the angular error is:

$$\sigma_\theta = 1.35°$$

The worst case for the angle estimates is for the smallest displacements.

EQUIPMENT AND EXPERIMENTAL SETUP

The particle images were recorded using a nominal 10 Watt cw argon-ion laser, operating in multiline mode, and an intensified, gated CCD array frame camera. The cw laser/intensified camera combination was chosen so that multiple exposures could be obtained on a microsecond time scale. The laser is capable of supplying 18 Watts of multiline output. The multiline output from the laser was formed into a light sheet by the three lenses shown in figure 3.

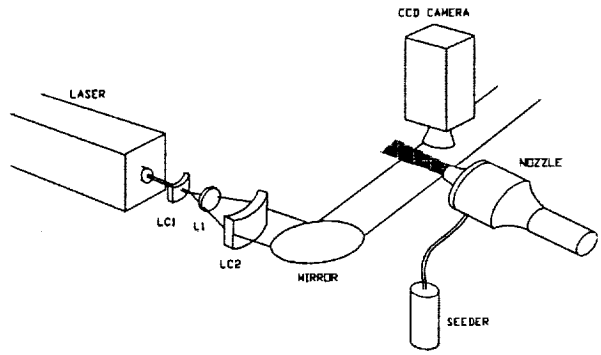

Figure 3: Schematic view of the experimental setup. The light sheet illuminates the centerline plane of the nozzle exit. The CCD camera is mounted above the nozzle looking downward.

Lenses LC_1 and LC_2 are cylindrical lenses of focal lengths 6 and 300 mm, respectively. Lens L_1 is a 600 mm focal length spherical achromat. The cylindrical lenses create a light sheet 50 mm wide. The lens L_1 is used as a mode match lens to propagate the beam waist from the laser to the probe volume.[19] The imaged area of the light sheet is approximately square, 50×50 mm. The beam thickness in the probe volume is approximately 0.5 mm, and increases by 8% at ± 25 mm from the waist location.

A sonic nozzle flow was used to demonstrate the high speed PDT technique. Figure 3 shows a diagram of the experimental configuration. The nozzle is a constant radius nozzle, with a radius of 19.05 mm. The nozzle flow was seeded in the nozzle plenum chamber with 1 μm Polystyrene Latex Spheres (PSL) entrained in ethanol. The nozzle flow was oriented parallel to the bench top. The laser light sheet was formed and transmitted across the centerline of the nozzle, parallel with the bench top. The intensified, gated CCD array camera was mounted above the nozzle flow with a downward view. An arbitrary waveform generator, controlled via the system computer, provided the gating pulse train to the CCD camera. The computer also contained the frame-grabber board used to digitize the imagery.

A XYBION ISG-250 frame camera, equipped with an

f/1.4, 25 mm focal length lens, was used to image the light scattered from the particles. The XYBION ISG-250 uses a Generation II image intensifier with a fiberoptic minifier bonded directly to a SONY XE-77 inter-line transfer CCD chip.[20] The CCD chip resolution is 768×493 pixels. The length of the exposures is controlled by a continuously variable control on the side of the camera. The integration interval length, δT, can be adjusted from 25 nsec to 16.6 msec. By definition, a frame transfer camera should integrate both of the interlaced video fields simultaneously for 1/30 second. The XYBION camera does not adhere to this definition precisely. The XYBION camera has been modified to provide a "Top-of-Frame" flag, which is TTL logic high for the first video field (odd), and logic low for the second video field (even). Figure 4 shows a timing diagram for the "Top-of-Frame" flag, the vertical drive line, and the integration periods for 3 successive video frames.

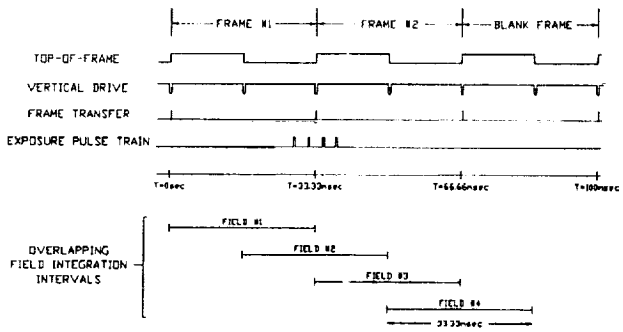

Figure 4: Timing diagrams indicating the drive signals from the CCD camera and the exposure pulse train. The field integration intervals are depicted in the bottom portion of the figure.

The vertical drive signal is normally a logic high, changing state to a logic low during the vertical blanking interval. The vertical drive signal remains low for 572.6 μseconds. The frame transfer pulse is an on-chip signal which terminates the integration period and initiates the transfer of the integrated video frame to a subregister for readout. The frame transfer pulse occurs 490 μsec into the vertical blanking interval.

In the XYBION camera, each video field is integrated for 33.3 msec, and the fields are read out of the camera every 16.6 msec, as per the RS-170 standard. The integration periods for the video fields are shown in the lower portion of figure 4. The odd and even field integration intervals overlap by 16.6 msec. Therefore, a full frame of video information is obtained only when the exposure occurs during the last 16.6 msec of the video integration period (when the even and odd field integration intervals overlap).

Two video frames of data are collected in the PDT data acquisition stage. Ideally, each frame would have completely independent exposures recorded on them. Figure 4 shows the exposure pulse train used to externally gate the CCD camera intensifier. To obtain two video frames with doubly exposed particle images on each, a four pulse exposure train is used. The exposure pulse train is centered about the frame transfer pulse in the vertical drive interval between frames 1 and 2. The first two pulses should cause the camera to record two exposures at the end of the frame #1 integration period. Similarly, the last two pulses should enable the camera to record two exposures at the start of the frame #2 integration interval. Hence, theoretically, frame #1 should contain two full video fields, as should frame #2. Unfortunately, this is not the case. Figure 4 shows two fields labeled 1 and 2 which belong to frame #1, and two fields labeled 3 and 4 which belong to frame #2. Video frame #1 will contain only one properly exposed video field, field #1, which stopped integrating at the end of frame #1. Field #2 in frame #2 continues integrating 16.6msec into frame #2. Field #3 begins integrating at the start of frame #2, and continues until the end of the frame. Field #4 starts 16.6 msec into frame #2, and ends 16.6ms into frame #3. The distribution of the recorded information is summarized in figure 5 for a sample interlaced particle image.

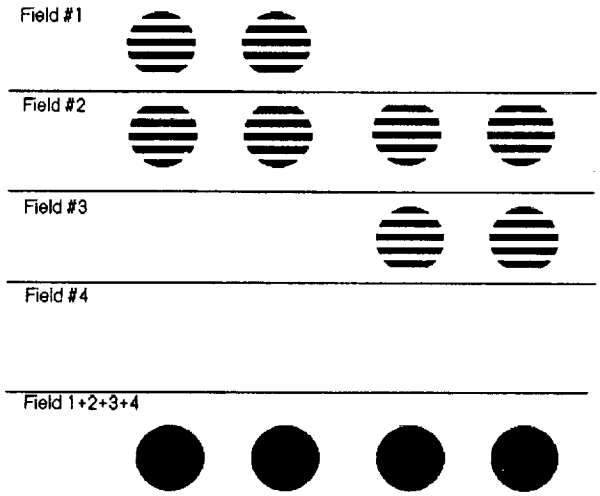

Figure 5: Graph illustrating the effects of gating the CCD frame camera across the frame transfer interval with overlapping field integration intervals.

Field #1 contains the odd lines of exposures 1 and 2. Field #2 contains the even lines for all four exposures. Field #3 contains the odd lines of exposures 3 and 4. No information has been recorded on field #4. By adding all four fields together, the complete set of recorded particle images is obtained.

Although the recorded exposures are not totally independent, sufficient information is available to decipher which particle images belong to which frame. To further complicate matters, the 2 exposures on field #1 leave a ghost image on field #3.

The enabling pulse train supplied to the camera intensifier gate input is created from a LeCroy 9100 arbitrary waveform generator. The time between pulses and the pulse width are nominally 10 μsec and 500 nsec, respectively. The "Top-of-Frame" signal from the camera is used as a trigger pulse for the waveform generator. The waveform generator delays the pulse train for approximately 30 msec so that the exposures are made near the end of the frame. The first two pulses enable the intensifier before the frame transfer pulse, and the last two pulses enable the intensifier just at the beginning of the next frame. The center of the pulse train must occur 295 μsec after

the leading edge of the "Top-of-Frame" pulse. The minimum time interval, ΔT, between the exposure pulses is 10 μsec. Smaller values of ΔT cause the exposure to occur within the frame transfer interval, which results in a very low level or non existent exposure. The waveform lasts for an additional 35 msec to ensure that a complete video frame elapses before the next "Top-of-Frame" pulse can retrigger the waveform generator. By suppressing the next exposure by a video frame period, any residual ghost images left in the CCD chip registers can be read out.

An EPIX 4-MEG video frame-grabber board digitizes and stores the multiply exposed PIV images.[21] The frame-grabber board A/D is equipped with a 12.5MHz oscillator so that interlaced 640×480×8bit square pixel frames are digitized. The resulting effective camera pixel size is 13.2 μm. The frame-grabber board can be configured to digitize individual fields or frames. In field mode the minimum sampling time is 1/60 second. When acquiring video fields, 27 fields can be acquired and stored in the 4Mbyte on-board memory buffer.

The EPIX frame-grabber board is configured to acquire individual video fields for the PDT data acquisition. Since the frame-grabber is not synchronized to the "Top-of-Frame" flag from the camera, a sequence of 8 fields is acquired. By analyzing the energy content of the 8 images, the software determines the three fields containing the exposures and saves them to disk.

The first step in reducing the particle image data is to determine the particle image centroids. The particle image centroids are computed by a boundary searching algorithm which determines the particle boundaries and then computes the centroid from an intensity weighted mean calculation.[15] The three video fields are added together to create a single 640×480 full resolution video frame. The particle centroids are computed using this summed frame. As each particle centroid is computed, the outlined area of the particle image boundary is used to compute the energy content of the same area on video field #1. If the energy content in the region in field #1 is greater than 0, then the particle image is assumed to have been recorded during the first two exposure pulses and is hence labeled as a frame #1 particle. If the region on field #1 contains zero energy, then the particle is assumed to have been recorded during the last two exposure pulses and labeled as a frame #2 particle. Field #1 is used to check the time order since field #3 will contain some ghost images from field #1. A single time history coded particle centroid image is generated which contains 640×480 pixels with amplitude 2^1 for particles from frame #1 and amplitude 2^2 for particles from frame #2. The time history image is then processed to determine the velocity vectors by the PDT algorithm discussed above.

The data acquisition and PDT processing are all performed on a 25MHz 80386 computer with a Weitek 3167 coprocessor. All of the PDT processing routines are written in Fortran 77 and compiled with a 32 bit Weitek supported compiler. The EPIX board data acquisition routines are written in C. Video images are stored on the hard disk and later transferred to removable cartridge disks for archiving.

RESULTS AND DISCUSSION

The experimental setup was first used to determine the size of the measured particles via the particle lag velocity. This test was performed to ensure that individual particles were being measured, not agglomerated particles. The sonic nozzle was operated at sonic conditions at pressure ratio of 0.5283.[22] The critical gas velocity at the nozzle exit was computed using the pressure ratio and the plenum temperature. The computed critical velocity for the nozzle flow at 21°C and ambient pressure of 14.26 psia was 314.5 m/s. The flow was seeded with 1 μm PSL particles which have a density of 1.05 gm/cc. The camera was operated in a continuous multi-gating mode using the arbitrary waveform generator to record approximately 15 exposures per video field. The time between exposures was 10 μsec and the integration interval was δT = 1.2 μsec. Figure 6 shows a sample multi-exposure image.

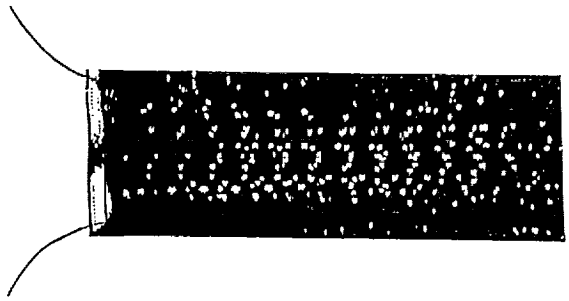

Figure 6: Multiply exposed image of particle seeded flow from the sonic nozzle. The particle lag velocity is used to verify the particle size. The inter-exposure time is 10 μsec.

The nozzle flow is from left to right and the nozzle position is indicated in the figure. The scale factor for the image is 72.5 μm/pixel. The recorded particle images are nominally 4 pixels in diameter. Considering diffraction effects, the imaged particle size at the camera sensor should be approximately 16 μm. Thus at the imaged field of view, the 1 μm particles should be imaged to just over a pixel. The intensifier/fiber optic minifier in the camera tends to bloom the particle images. The relatively long exposure times, δT, did not produce streaked particle images. At a velocity of 100 m/s, the particles move approximately 100 μm during the exposure, which is still on the order of the pixel imaging area. The diffraction and camera blooming effects mask any streak effects. The particle velocities were determined by manually estimating the particle centroids at successive downstream locations. Table I shows the measured particle velocities as a function of axial position.

The axial position where the particle velocity exceeds the computed critical velocity is used to determine the particle size. The axial location where the particle reaches the critical velocity is between 1.0 and 1.16 normalized axial coordinates. Figure 7 shows a graph of computed particle lag velocities versus axial position.

Normalized Axial Position	Particle Velocity [m/s]
0.34	289.9
0.50	304.4
0.67	311.6
0.83	318.8
1.00	311.6
1.16	318.8
1.33	318.8
1.50	318.8

Table I Measured particle lag velocities at successive axial positions down stream from the nozzle exit plane. The axial positions are normalized by the nozzle radius of curvature. The particle reaches the gas velocity at approximately 1 nozzle radii of curvature downstream.

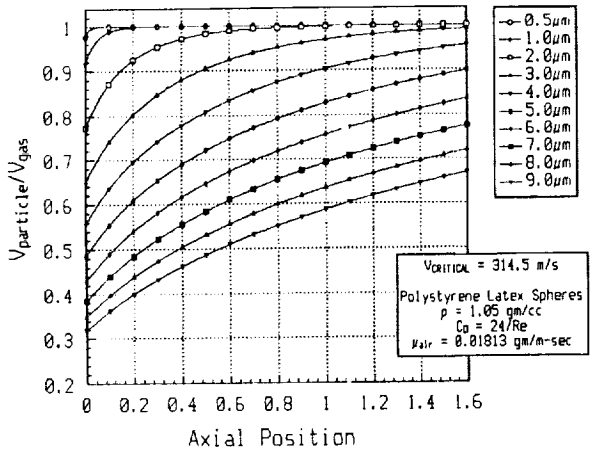

Figure 7: Graph of particle lag velocity versus axial position. The axial position is normalized by the nozzle radius of curvature (19.1 mm).

The axial positions are normalized by the nozzle radius of curvature. The particle lag velocities were computed by finite differencing the particle dynamics equations from the nozzle plenum to 1.6 normalized axial coordinates downstream of the nozzle.[23] Particle lag velocities for PSL particles from 0.5 up to 9.0 μm were computed and are shown in the figure. By examining the graph, a particle whose velocity reaches the gas velocity at approximately 1.0 nozzle radii of curvature downstream should be 2 μm in diameter. Thus, the PSL particles used in this study are approximately 1-2 μm in diameter. The discrepancy in the measured particle size can be attributed to particle agglomeration. The particles were not specially treated before use to minimize agglomeration. The particle lag velocity test was performed only to ensure that approximately 1 μm particles were measured, not severely agglomerated particles.

Having verified that the measured particles were on the order of 1-2 μm, the high speed velocity measurements were conducted. The sonic nozzle was operated above the design pressure ratio of 0.5283. The laser was operated at 18Watts multiline, continuous wave. The CCD camera was operated at the minimum inter-pulse interval of ΔT = 10 μsec from the waveform generator. The camera integration period, δT, was set to 1.5 μsec. The seed particle density was fairly low. The recorded particle image tracks were well separated from each other. The ambient temperature and pressure were 22.1°C and 14.4 psia, respectively. The camera field of view was approximately 48×36 mm. The corresponding velocity scale is:

$$V_{scale} = \frac{74.4\mu m/pixel}{3\times\Delta T} = 2.48 m/s\cdot pixel$$

Figures 8 and 9 show the measured velocity vectors for two different pressure ratios of 0.95 and 0.89, respectively. In each figure, there are 2 groups of five frames of data displayed.

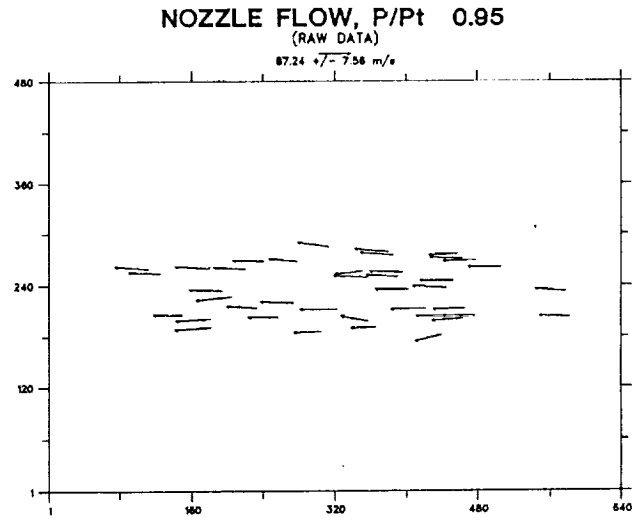

Figure 8: Graph of the measured velocity vectors from the nozzle operating at a pressure ratio P/P_t = 0.95. The computed exit velocity is 91 m/s.

The frame-grabber acquisition software is designed to acquire an extended sequence of fields and divide them up into the appropriate groups of 3. A total of 15 exposed fields are saved to disk. Each group of 3 fields is used to generate a single velocity vector map. Hence, five frames of data are generated by the processing software. The number of detected velocity vectors is low, due to the low seeding density. The field of view lies approximately 5 nozzle diameters downstream. Figure 8 contains 40 velocity vectors with a mean velocity of 87.4 m/s and a standard deviation of ±7.5 m/s. From the operating pressure ratio of 0.95, the computed velocity is 91 m/s. The average particle displacement between exposures is roughly 12 pixels. From the average displacement, the predicted error in the menasured velocities via equation 3 is

1.7 m/s, which is well below the measured flow fluctuations. The measured variation in the mean velocity is higher than predicted due to the downstream mixing effects in the nozzle flow. Figure 9 contains 37 velocity vectors with a mean velocity of 138.5 m/s and a standard deviation of 9.9 m/s.

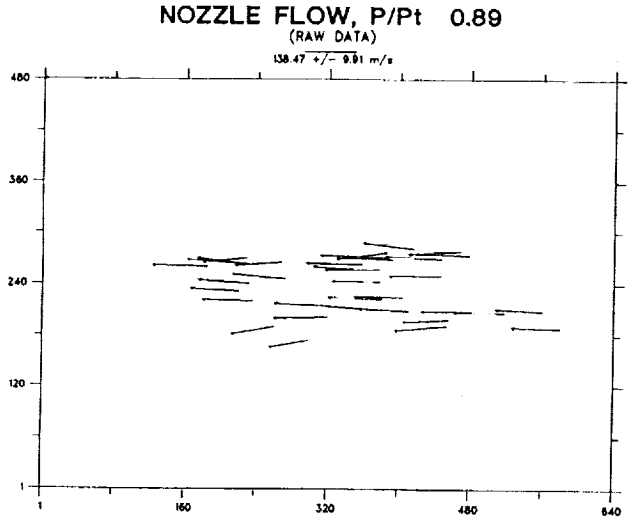

Figure 9: Graph of the measured velocity vectors from the nozzle operating at a pressure ratio $P/P_t = 0.89$. The computed exit velocity is 138.6 m/s.

For this data set, the operating pressure ratio was 0.89, which corresponds to a critical velocity of 138.6 m/s. The average particle displacement between exposures is approximately 19 pixels. The total processing time for the data displayed in figures 8 and 9 is approximately 40 seconds each. The boundary processing and PDT processing individually require roughly 2 CPU seconds/frame.

The PDT technique has a relatively low dynamic range sensitivity since the particle images cannot overlap on the doubly exposed images. The dynamic range for 12 pixel displacements between exposures and 4 pixel wide particles is roughly 3:1 The data are easily acquired and a wider dynamic range may be achieved by acquiring successive data sets with varied inter-exposure times to produce the desired velocity sensitivity. The velocity measurement range of the PDT technique for a 50×50 mm field of view is determined by the minimum and maximum inter-exposure intervals of 10 msec and 10 μsec, respectively. The measurable velocity range is from 0.1 m/s to 150 m/s.

CONCLUSIONS

The PDT technique is an all electronic PIV data acquisition and reduction system. Previous application of the PDT technqiue was limited to low velocity liquid flows. The newly modified high speed version of the PDT technique is capable of measuring velocities from 0.1 to 150 m/s. The PDT technique employs a single gated, intensified camera and a cw laser source to record microsecond exposures. Directionally resolved particle velocities are measured. All of the data acquisition and processing is performed on a 25MHz 80386 computer. Processing times are on the order of seconds. Although the preliminary data presented here were recorded with a very low particle seeding density, higher particle seeding densities are possible. The maximum measurable velocity is physically limited by the frame transfer characteristics of the RS-170 yideo CCD chip used to record the images. Future application of the PDT technique will investigate the use of a high per pulse energy spark gap light source and a standard CCD array camera. Use of a small size spark gap light source will minimize space requirements and ease system integration into aerospace facilities.

REFERENCES

1) Meynart, R.;"Instantaneous Velocity Field Measurements in Unsteady Gas Flow by Speckle Velocimetry", *Appl. Opt.* **22**, 535-540 (1983).

2) R. J. Adrian, C. S. Yao,"Pulsed Laser Technique Application to Liquid And Gaseous Flows And The Scattering Power of Seed Materials", *Appl. Opt.* **24**, 44-52 (1985).

3) L. Lourenco, A. Krothapalli,"Particle Image Displacement Velocimetry Measurements of a Three-Dimensional Jet", *Phys. Fluids* **31**, 1835-1837 (1988).

4) R. J. Adrian, C. S. Yao,"Development of Pulsed Laser Velocimetry (PLV) for Measurement of Fluid Flow", in *Proceedings, Eighth Biennial Symposium on Turbulence*, X. B. Reed, Jr., J. L. Kakin, and G. K. Patterson, Eds., 170-186 (U. Missouri Rolla 1983).

5) R. Höcker, J. Kompenhans,"Application of Particle Image Velocimetry to Transonic Flows", *5th International Symposium on Applications of Laser Anemometry to Fluid Mechanics*, Lisbon, Portugal, paper #15.1, (1990).

6) L. P. Goss, M. E. Post, D. D. Trump, B. Sarka, C. D. MacArthur, G. E. Dunning, Jr.,"A Novel Technique for Blade-to-Blade Velocity Measurements in a Turbine Cascade", *25th Joint Propulsion Conference*, AIAA-89-2691, (1989).

7) P. J. Bryanston-Cross, A. H. Epstein,"The Application of Submicron Particle Visualisation for PIV (Particle Image Velocimetry) at Transonic Speeds", *Progress in Aerospace Science*, 1-31, Oct., (1990).

8) Y. C. Cho, B. G. McLachlan,"Personal Computer Based Image Processing Applied to Fluid Mechanics Research", *SPIE Applications of Digital Image Processing* **829**, 253-257 (1987).

9) K. A. Marko, L. Rimai,"Video Recording and Quantitative Analysis of Seed Particle Track Images in Unsteady Flows", *Appl. Opt.* **24**, 3666-3672 (1985).

10) A. A. Adamczyk, L. Rimai,"2-Dimensional Particle Tracking Velocimetry (PTV): Technique and Image Processing Algorithms", *Experiments in Fluids*, **6**, 373-380, (1988).

11) B. Khalighi, Y. H. Lee,"Particle Tracking Velocimetry: An Automatic Image Processing Algorithm", *Appl. Opt.* **28**, 4328-4332 (1989).

12) B. R. Frieden, C. K. Zoltani,"Fast Tracking Algorithm for Multiframe Particle Image Velocimetry Data", *Appl. Opt.* **28**, 652-655 (1989).

13) Y. Hassan, T. Blanchat,"Two-Phase Flow Velocity Measurements Using Automated-Based Imaging Pulsed Laser Velocimetry", *5th International Symposium on Applications of Laser Anemometry to Fluid Mechanics*, Lisbon, Portugal, paper #18.5, (1990).

14) Y. C. Cho,"Digital Image Velocimetry", *Appl. Opt.* **28**, 740-748 (1989).

15) M. P. Wernet,"A New Data Reduction Technique for Pulsed Laser Velocimetry", Ph.D. Thesis, Case Western Reserve University, May (1989).

16) M. P. Wernet, R. V. Edwards,"A New Space Domain Processing Technique for Pulsed Laser Velocimetry", *Appl. Opt.* **29**, 3399-3417 (1990).

17) M. P. Wernet,"Particle Displacement Tracking (PDT) for PIV", NASA TM-103288, Sept., (1990).

18) LeCroy 9100 Arbitrary Waveform Generator Operator's Manual, October, (1988).

19) R. G. Seasholtz,"Laser Doppler Velocimeter System for Turbine Stator Cascade Studies and Analysis of Statistical Biasing Errors", NASA TN D-8297, (1977).

20) XYBION ISG-250 Camera Operator's Manual, (1989).

21) EPIX 4-MEG Video Board Operator's Manual, (1989).

22) Ames Research Staff, "Equations, Tables, and Charts For Compressible Flow", NACA Report 1135, (1953).

23) B. R. Maxwell, R. G. Seasholtz, "Velocity Lag of Solid Particles in Oscillating Gases and in Gases Passing Through Normal Shock Waves", NASA TN D-7490, (1974).

NASA
National Aeronautics and Space Administration

Report Documentation Page

1. Report No.	2. Government Accession No.	3. Recipient's Catalog No.
NASA TM-104481		

4. Title and Subtitle	5. Report Date
Particle Displacement Tracking Applied to Air Flows	
	6. Performing Organization Code

7. Author(s)	8. Performing Organization Report No.
Mark P. Wernet	E-6329
	10. Work Unit No. 505-62-50

9. Performing Organization Name and Address	11. Contract or Grant No.
National Aeronautics and Space Administration Lewis Research Center Cleveland, Ohio 44135-3191	
	13. Type of Report and Period Covered: Technical Memorandum

12. Sponsoring Agency Name and Address	14. Sponsoring Agency Code
National Aeronautics and Space Administration Washington, D.C. 20546-0001	

15. Supplementary Notes

Prepared for the Fourth International Conference on Laser Anemometry cosponsored by the American Society of Mechanical Engineers and the European Association for Laser Anemometry with organizational collaboration and sponsorship from Case Western Reserve University, Cleveland State University, NASA Lewis Research Center, and the Ohio Aerospace Institute, Cleveland, Ohio, August 5-9, 1991. Responsible person, Mark P. Wernet, (216)433-3752.

16. Abstract

Electronic Particle Image Velocimetric (PIV) techniques offer many advantages over conventional photographic PIV methods such as fast turn around times and simplified data reduction. A new all electronic PIV technique has been developed which can measure high speed gas velocities. The Particle Displacement Tracking (PDT) technique employs a single cw laser, small seed particles (1μm), and a single intensified, gated CCD array frame camera to provide a simple and fast method of obtaining two-dimensional velocity vector maps with unambiguous direction determination. Use of a single CCD camera eliminates registration difficulties encountered when multiple cameras are used to obtain velocity magnitude and direction information. An 80386 PC equipped with a large memory buffer frame-grabber board provides all of the data acquisition and data reduction operations. No array processors or other numerical processing hardware are required. Full video resolution (640x480 pixel) is maintained in the acquired images, providing high resolution video frames of the recorded particle images. The time between data acquisition to display of the velocity vector map is less than 40 seconds. The new all electronic PDT technique is demonstrated on an air nozzle flow with velocities <150 m/s.

17. Key Words (Suggested by Author(s))	18. Distribution Statement
Particle trajectories Velocity measurement	Unclassified - Unlimited Subject Category 35

19. Security Classif. (of the report)	20. Security Classif. (of this page)	21. No. of pages	22. Price*
Unclassified	Unclassified	10	A02

*For sale by the National Technical Information Service, Springfield, Virginia 22161